RAPID COMMUNICATIONS IN MASS SPECTROMETRY
Rapid Commun. Mass Spectrom. 2007; **21**: 1304–1314
Published online in Wiley InterScience (www.interscience.wiley.com) DOI: 10.1002/rcm.2962

Rapid measurement of sphingolipids from *Arabidopsis thaliana* by reversed-phase high-performance liquid chromatography coupled to electrospray ionization tandem mass spectrometry

Jonathan E. Markham* and Jan G. Jaworski
Donald Danforth Plant Science Center, St. Louis, Missouri, USA

Received 4 December 2006; Revised 19 January 2007; Accepted 2 February 2007

Changes in sphingolipids have been associated with profound effects in cell fate and development in both plants and animals. Sphingolipids as a group consist of a large number of different compound classes of which numerous individual species may vary in response to environmental stimuli to affect cellular responses. The ability to measure all sphingolipids simultaneously is, therefore, essential to an understanding of the biochemical regulation of sphingolipid metabolism and signaling molecules derived from it. In the model plant *Arabidopsis thaliana*, the major sphingolipid classes are glycosylinositolphosphoceramides, glucosylceramides, hydroxyceramides and ceramides. Other minor but potentially important sphingolipids are free long-chain bases and their phosphorylated derivates. By using a single solvent system with reversed-phase high-performance liquid chromatography coupled to electrospray ionization tandem mass spectrometry detection we have been able to separate and measure 168 sphingolipids from a crude sample. This greatly speeds up and simplifies the analysis of plant sphingolipids and should pave the way for a better understanding of their role in plant performance. Copyright © 2007 John Wiley & Sons, Ltd.

There are numerous, potent ways in which sphingolipids may affect the fate of plant cells. Complex sphingolipids such as glycosylinositolphosphoceramides (GIPCs) and glucosylceramides(GlcCers) have been implicated in the formation of plasma membrane microdomains known as 'lipid rafts' and may directly affect the intercellular sorting of vital proteins.[1,2] Changes in the level of ceramides (Cers) have been shown to be directly associated with programmed cell death in the accelerated cell death mutant *acd*5.[3] An increase in free long-chain bases (LCBs) and disruption of sphingolipid biosynthesis occurs in the AAL-toxin or fumonisin B_1 induced programmed cell death in tomato,[4–6] and long-chain base phosphates (LCBPs) stimulate the closure of guard cells to prevent water loss during drought.[7] As in animals, this wide range of effects has been suggested to result from a rheostat-type mechanism where interplay between different components of sphingolipid metabolism combine to produce the ultimate effect.[6,8,9] It is essential, therefore, to understand how the entire sphingolipid content or sphingolipidome changes to produce the final biological outcome.[9]

Plant sphingolipids are structurally complex, having numerous possible combinations of fatty acids, desaturations, hydroxylations and head groups and have a broad range of cellular concentrations.[10,11] Measuring this wide array of compounds from within a crude sample is only realistically possible with current technology using mass spectrometry (MS).[12] MS is able to selectively measure target compounds from within a mixture by using unique parameters for each analyte of choice thereby ignoring the non-target contaminants. Due to the complexity of plant sphingolipids, however, and limitations of the technology, MS alone may not achieve the resolution necessary to sufficiently distinguish between levels of desaturation and sites of hydroxylation. This is particularly true for compounds of higher molecular weight where the diisotopic forms of unsaturated compounds complicate the signal for saturated compounds and for compounds where fragmentation does not reveal all structural details. Hence, coupling the sensitivity and specificity of the mass spectrometer to the equally powerful and analytical technique of high-performance liquid chromatography doubles the resolving power of the analysis and provides robust levels of analyte identification.

Arabidopsis thaliana is the model plant of choice for plant biologists and contains a relatively simple complement of sphingolipid classes, GIPCs, GlcCers, Cers, hydroxy-Cers, LCBs and LCBPs.[11] We have developed high-performance liquid chromatography/electrospray ionization tandem mass spectrometry (HPLC/ESI-MS/MS) methods sufficient for the measurement of 168 sphingolipids from across these classes starting from a small amount of sample material. The technique greatly decreases the time required for analysis

**Correspondence to*: J. E. Markham, Donald Danforth Plant Science Center, 975 N Warson Rd, St. Louis, MO 63132, USA.
E-mail: jmarkham@danforthcenter.org
Contract/grant sponsor: NSF Arabidopsis 2010 Grant; contract/grant number: MCB 0312559.

enabling high-throughput monitoring of plant sphingolipids.

EXPERIMENTAL

Materials

Except where noted, all chemicals were of HPLC grade or highest grade available from Sigma Aldrich (St. Louis, MO, USA). Methanol and tetrahydrofuran (THF) were Omnisolv grade obtained from EMD Biosciences (San Diego, CA, USA). Propan-2-ol was HPLC grade and hexanes were optima grade both obtained from Fisher Scientific (Pittsburgh, PA, USA).

Internal standards

Standards for quantification of sphingolipids were purchased from Avanti Polar Lipids Inc. (Alabaster, AL, USA). Standards were dissolved at 1 mg/mL in chloroform/methanol/water (16:16:5 v/v/v). Individual standards were combined in a 2 mL HPLC vial in the following quantities: GM1 (ovine), 200 nmol; C12-GlcCer, 100 nmol; C12-Cer, 10 nmol; sphingosine (C17 base), 10 nmol; and sphingosine-1-phosphate (C17 base), 10 nmol. The solvent was evaporated by a gentle stream of nitrogen and the standards dissolved in 1000 μL of extraction solvent (lower phase of isopropanol/hexane/water (55:20:25 v/v/v)) and stored at −30°C until required. Exact concentrations of internal standards in each batch were checked by diluting 10 μL of standard to 990 μL with THF/methanol/water (2:1:2 v/v/v) containing 0.1% formic acid and running the sample through the HPLC/MS system. The absolute amount of each standard was then calculated based on the standard curves (see below).

Sample preparation

Approximately 30 mg of freeze-dried Arabidopsis tissue was weighed into a 3 mL DUALL glass tissue grinder (Kontes, Vineland, NJ, USA) to which 10 μL of internal standards and 3 mL of extraction solvent were added. The tissue was fully homogenized with the glass plunger of the DUALL tissue grinder, attached to a Ryobi D45CK power drill rotating at up to 1000 rpm. When homogenization was complete, the sample was transferred to a 10 mL glass centrifuge tube. The tissue grinder was rinsed with an additional 2 mL of extraction solvent which was added to the homogenate, after which the tube was capped and incubated at 60°C for 15 min. After centrifugation at 500 *g* for 10 min the supernatant was decanted to a second tube and the pellet extracted once more with 3 mL of extraction solvent. After a second incubation at 60°C for 15 min and centrifugation as before, the supernatants were combined and dried under a stream of nitrogen. The dried, crude extract was deesterified by dissolving in 2 mL of 33% methylamine solution in ethanol/water (7:3 v/v) and incubating at 50°C for 1 h. After hydrolysis the sample was dried under nitrogen and dissolved with heating and gentle sonication in 1 mL of THF/methanol/water (2:1:2 v/v/v) containing 0.1% formic acid. The sample was spun at 500 *g* for 10 min to remove any insoluble material, transferred to an autosampler vial and stored at −30°C until analysis.

Mass spectrometry

Purified sphingolipids and standards were directly infused into the TurboIonSpray source of a 4000 QTRAP® LC/MS/MS System (Applied Biosystems, Foster City, CA, USA) using a KDS100 syringe pump (KD Scientific Inc., Holliston, MA, USA) at 10 μL min^{-1} with a needle temperature of 100°C, needle voltage +5000V, curtain gas 10 psi, nebulizing gas (GS1) 20 psi, focusing gas (GS2) 0 psi, and the interface heater was engaged. Declustering potential (DP) and collision energy (CE) were optimized on a compound-dependent basis.

HPLC/ESI-MS/MS

The HPLC system consisted of two Shimadzu LC-20AB pumps connected to a HTC PAL autoinjector (CTC Analytics, Zwingen Switzerland) fitted with a 50 μL sample loop, a 100 μL X-type syringe and a fast wash station with two wash solvents: wash 1, isopropanol/hexane/water (55:5:25 v/v/v) + 0.5% triethylamine, 0.7% formic acid; and wash 2, THF/methanol/water (2:1:2 v/v/v) + 0.1% formic acid. Flow from the sample injector led to a 150 × 3 mm, 5 μm particle size, SUPELCOSIL ABZ+Plus column fitted with a guard cartridge held at 40°C in a Shimadzu CO-20A oven. The sample was eluted at 1 mL min^{-1} with a binary gradient system consisting of solvent A, THF/methanol/5 mM ammonium formate (3:2:5 v/v/v) + 0.1% formic acid, and solvent B, THF/methanol/5 mM ammonium formate (7:2:1 v/v/v) + 0.1% formic acid (see Table 2 for gradient details). The initial eluate from the column was directed via a Valco valve to waste for 1.4 min after which the flow was switched to the TurboIonSpray source of the 4000 QTRAP® LC/MS/MS system. The probe was vertically positioned 11 mm from the orifice and charged with 5000 V. The temperature was held at 650°C, GS1 was set at 90 psi, GS2 at 50 psi, curtain gas at 20 psi, and the interface heater was engaged.

Calibration of MS/MS detection

Serial dilutions were constructed in triplicate for each standard and unknown starting from approximately 200 pmol/μL for GIPCs/GM_1; 100 pmol/μL for GlcCers/C12-GlcCer; and 10 pmol/μL for Cer/C12-Cer, LCBs/d17:1 and LCBPs/d17:1-P. The concentration of sphingolipid in each of the first three dilutions was confirmed by removing the equivalent of 1 nmol of sphingolipid, hydrolyzing with barium hydroxide/dioxane, and quantifying the liberated LCBs as previously described.[11] The concentration of free LCBs and LCBPs was confirmed by by AccQ derivitization, HPLC and fluorescence detection as previously described.[13]

Data collection and analysis

Data was collected with the Analyst 1.4.2 software (Applied Biosystems). Peaks for individual sphingolipids were assigned based on elution time of known standards and by comparison with other peaks. Peaks were integrated using the Intelliquan algorithm with a minimum of three rounds of smoothing and a bunching factor of 2. Smoothing and bunching factor were adjusted on a peak-by-peak basis to ensure adequate peak identification. Peak area was used to determine the relative ratio of each peak compared to the

DOI: 10.1002/rcm

RCM

added internal standard, multiplied by the total amount of internal standard added (in nmol) and divided by the amount of starting tissue (in g) to give a value of nmol sphingolipid/g dry weight (dw).

RESULTS

Optimization of mass spectrometer parameters

In order to monitor the elution of sphingolipids from the HPLC column and provide a measure of their abundance, the multiple-reaction monitoring (MRM) mode of the 4000 QTRAP mass spectrometer was used. In this mode, the machine monitors for specific precursor-product ion pairs with conditions optimized for each reaction. By rapidly switching between states the machine is able to monitor numerous reactions at once. This required the construction of detailed MRM tables with parameters for each compound being analyzed.

Purified sphingolipids from Arabidopsis were used to establish the parameters for MRM. For each class of sphingolipid, the purified compounds were introduced by infusion and the major ions identified. These ions were fragmented at increasing collision energies to produce an array of all possible fragments. An optimization MRM table was then constructed based on these fragments (not shown). Using the 'ramp' feature of the Analyst software, declustering potential (DP) and collision energy (CE) were systematically varied to identify the precursor-product ion reaction for each compound class that gave the highest sensitivity. The precursor-product ion transitions chosen for each class of sphingolipid are detailed in Fig. 1. For neutral sphingolipids and LCB(P)s, the fragmentation typically resulted in detection of a product ion containing the LCB portion of the molecule. For charged sphingolipids, choosing this ion fragment significantly reduced the sensitivity and thus, for the GIPCs, the ceramide fragment was chosen. This resulted in some loss of structural information which reduced the ability to distinguish some analytes as they had identical precursor-product ion transitions. This was overcome by using retention time to differentiate such analytes (see below). Although GIPCs naturally carry a negative charge, it was found that with the acidic HPLC solvents the positively charged species was detectable with greater sensitivity (data not shown). In addition, positive mode was required in order to detect the ceramide fragment ion and achieve the best identification.

Once a precursor-product ion transition had been chosen, a final MRM table was constructed for 40 different LCB/fatty acid combinations within each class and for eight LCB/LCB(P) combinations (Tables 1(A)–1(E)). The 'ramp' feature was again employed, this time to optimize the DP and CE for each transition that gave the maximum signal. Once the mass spectrometer parameters had been optimized, a 'T'-connection was used to combine the flow from the HPLC system with the flow from the infusion pump and optimize the source parameters. Finally, the purified sphingolipids were injected, along with the appropriate standard, onto the HPLC column, and suitable gradient programs constructed for each class (Table 2) that provided sufficient separation of peaks for individual species by acyl-chain length and desaturation to allow rigorous identification.

Detection of sphingolipids in a crude extract

Due to their highly amphiphilic nature, plant sphingolipids are best extracted into an isopropanol/hexane/water mixture.[11] Sphingolipids are resistant to mild-base hydrolysis which is often performed to reduce interference from other lipid compounds during HPLC, ESI and detection. Typically, this is done with 0.1 N NaOH which is removed prior to HPLC by extraction of sphingolipids into chloroform. This is not an effective approach with plant sphingolipids as GIPCs are poorly soluble in chloroform. Instead, lipids were hydrolyzed with monomethylamine, a volatile, mild base capable of hydrolyzing ester-containing lipids (e.g. phospholipids) but not sphingolipids.[14,15]

Internal standards were added during the preparation of the extract. For accurate quantification by mass spectrometry standards should be as close in structure and properties to the compound being detected as possible. However, differences in chemistry between the standards and unknowns being quantified meant a calibration factor was required to establish the molar relationship between the analytes and the standards.

Calibration of mass spectrometer response

Although mass spectrometers have a large theoretical dynamic range, in practice their response may only be linear across a smaller portion of that range. To determine the linear range of detector response, standard curves consisting of a 1×10^5 dilution of standard and purified unknown compounds were generated. The concentration of sphingolipid for each standard curve was independently verified by making fluorescent derivatives of hydrolyzed sphingolipids and quantifying the LCBs by HPLC. For the majority of sphingolipid species, the results showed a distinctly sigmoid curve indicating that quantification was only possible within a defined range. Within that range, however, the response of each sphingolipid was linear and proportional to the standard. It was found that linear ranges for individual sphingolipid species were broadly within signal intensities of 10^4 to 10^7 allowing for a 1000 × fold change in sphingolipid levels to be measured. Outside of this range the response was non-linear both for the standard and the unknowns and therefore tended to overestimate or underestimate the amount of sphingolipid.

The ideal standard for each sphingolipid species to be measured is a compound with identical chemistry that varies by enough mass units to be distinguishable from the unknown to be measured. Synthetic standards with a C17 LCB or C12 fatty acid component make reasonable standards; however, commercially available sphingolipid standards are usually available with a d18:1Δ4 LCB which are not chemically the same as sphingolipid species found in plants, which typically contain a t18:1Δ8 LCB.[16] Furthermore, no commercially available plant GIPC standard was available and costly synthesis of such a standard could potentially be avoided if a suitable substitute could be found; in these experiments the negatively charged

DOI: 10.1002/rcm

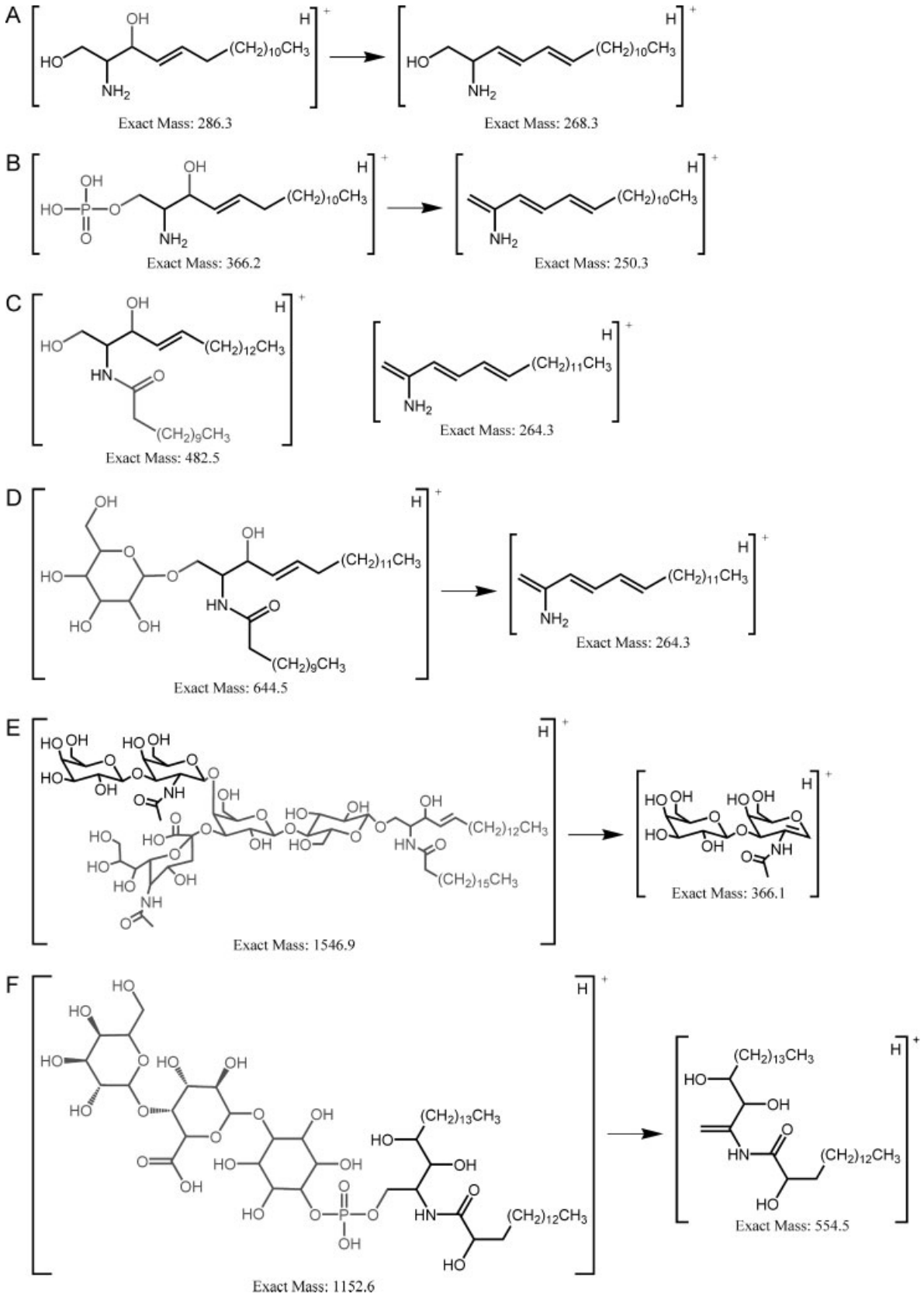

Figure 1. Fragmentation of sphingolipid and sphingolipid standards. The precursor and product ion fragment used for the measurement of sphingolipids in this work is shown. Atoms lost from the precursor ion are shown in grey, hydrogen transfers are assumed and no mechanism is implied. Other isomeric structures may be plausible. LCB and fatty acid nomenclature are as follows, LCB; d/t (di/trihydroxy) 18 (18 carbon chain): 1 (one desaturation) followed by fatty acid; c/h (non-hydroxy/hydroxy) 12 (12 carbon chain): 0 (no desaturations). Fragmentation of (A) LCBs (d17:1 shown); (B) LCB-Ps (d17:1-P shown); (C) ceramides (d18:1c12:0 shown); (D) GlcCers (C12-GlcCer shown); (E) ganglioside GM_1; and (F) GIPCs (t18:0h16:0 shown).

DOI: 10.1002/rcm

RCM

Table 1. Parameters for MRM detection of sphingolipid classes. Parameters for precursor and product ions were determined by calculation of the exact mass (to 1 decimal place) based on known structures and the observed fragmentation patterns detailed in Fig. 1. Dwell time was set to allow at least one observation for each analyte per second. Optimum declustering potential (DP), collision energy (CE) and elution time (ET) were determined empirically

Analyte	$[M+H]^+$ (*m*/*z*)	Product ion (*m*/*z*)	Dwell time (ms)	DP (V)	CE (V)	ET (min)
(A) LCBs and LCBPs						
d17:1	286.3	268.3	20	55	16	3.72
t18:0	318.3	300.4	20	70	21	4.24
t18:1	316.3	298.4	20	60	18	3.73
d18:1	300.3	282.3	20	65	18	4.45
d18:0	302.3	284.3	20	75	21	4.87
d17:1-P	366.2	250.3	20	60	23	2.47
t18:0-P	398.3	300.3	20	65	22	3.01
t18:1-P	396.3	298.3	20	60	25	2.63
d18:0-P	382.3	266.3	20	65	19	3.31
d18:1-P	380.3	264.3	20	60	25	3.03

LCB	Fatty acid	[M+H] (*m*/*z*)	Product ion (*m*/*z*)	Dwell time (ms)	DP (V)	CE (V)	ET (min)
(B) Ceramides							
d18:1	c12:0	482.5	264.3	19.39	60	35	5.06
t18:0	c16:0	556.5	300.3	19.39	100	35	6.73
t18:0	c18:0	584.6	300.3	19.39	100	35	7.92
t18:0	c20:0	612.6	300.3	19.39	100	37	9.14
t18:0	c20:1	610.6	300.3	19.39	100	37	7.55
t18:0	c22:0	640.6	300.3	19.39	100	43	10.4
t18:0	c22:1	638.6	300.3	19.39	100	43	8.94
t18:0	c24:0	668.7	300.3	19.39	100	43	11.5
t18:0	c24:1	666.7	300.3	19.39	100	43	10.3
t18:0	c26:0	696.7	300.3	19.39	100	43	12.6
t18:0	c26:1	694.7	300.3	19.39	100	43	11.4
t18:1	c16:0	554.5	298.3	19.39	100	38	6.27
t18:1	c18:0	582.6	298.3	19.39	100	38	7.52
t18:1	c20:0	610.6	298.3	19.39	100	40	8.70
t18:1	c20:1	608.6	298.3	19.39	100	40	8.15
t18:1	c22:0	638.6	298.3	19.39	100	42	9.92
t18:1	c22:1	636.6	298.3	19.39	100	42	9.39
t18:1	c24:0	666.7	298.3	19.39	100	42	11.1
t18:1	c24:1	664.7	298.3	19.39	100	44	9.84
t18:1	c26:0	694.7	298.3	19.39	100	44	12.2
t18:1	c26:1	692.7	298.3	19.39	100	44	11.0
d18:0	c16:0	540.5	266.3	19.39	40	42	7.74
d18:0	c18:0	568.6	266.3	19.39	40	43	8.99
d18:0	c20:0	596.6	266.3	19.39	42	43	10.2
d18:0	c20:1	594.6	266.3	19.39	40	48	8.83
d18:0	c22:0	624.6	266.3	19.39	39	48	11.4
d18:0	c22:1	622.6	266.3	19.39	40	48	10.3
d18:0	c24:0	652.7	266.3	19.39	39	44	12.5
d18:0	c24:1	650.7	266.3	19.39	37	43	11.3
d18:0	c26:0	680.7	266.3	19.39	43	48	13.5
d18:0	c26:1	678.7	266.3	19.39	46	48	12.4
d18:1	c16:0	538.5	264.3	19.39	40	39	7.25
d18:1	c18:0	566.6	264.3	19.39	38	39	8.53
d18:1	c20:0	594.6	264.3	19.39	44	39	9.78
d18:1	c20:1	592.6	264.3	19.39	42	42	8.42
d18:1	c22:0	622.6	264.3	19.39	44	46	11.0
d18:1	c22:1	620.6	264.3	19.39	39	44	9.64
d18:1	c24:0	650.7	264.3	19.39	38	49	12.1
d18:1	c24:1	648.7	264.3	19.39	42	43	10.6
d18:1	c26:0	678.7	264.3	19.39	38	46	13.1
d18:1	c26:1	676.7	264.3	19.39	46	48	11.7

LCB	Fatty acid	[M+H] (*m*/*z*)	Product ion (*m*/*z*)	Dwell time (ms)	DP (V)	CE (V)	ET (min)
(C) Hydroxyceramides							
d18:1	c12:0	482.5	264.3	19.39	60	35	4.92
t18:0	h16:0	572.5	300.3	19.39	100	36	6.05

(*Continues*)

DOI: 10.1002/rcm

Table 1. (Continued)

LCB	Fatty acid	[M+H] (*m*/*z*)	Product ion (*m*/*z*)	Dwell time (ms)	DP (V)	CE (V)	ET (min)
t18:0	h18:0	600.6	300.3	19.39	100	38	7.30
t18:0	h20:0	628.6	300.3	19.39	100	38	8.43
t18:0	h20:1	626.6	300.3	19.39	100	44	7.50
t18:0	h22:0	656.6	300.3	19.39	100	45	9.66
t18:0	h22:1	654.6	300.3	19.39	100	45	8.46
t18:0	h24:0	684.7	300.3	19.39	100	45	10.8
t18:0	h24:1	682.7	300.3	19.39	100	45	9.59
t18:0	h26:0	712.7	300.3	19.39	100	46	11.9
t18:0	h26:1	710.7	300.3	19.39	100	45	10.7
t18:1	h16:0	570.5	298.3	19.39	100	36	5.67
t18:1	h18:0	598.6	298.3	19.39	100	36	6.81
t18:1	h20:0	626.6	298.3	19.39	100	38	8.01
t18:1	h20:1	624.6	298.3	19.39	100	38	6.96
t18:1	h22:0	654.6	298.3	19.39	100	43	9.24
t18:1	h22:1	652.6	298.3	19.39	100	43	8.04
t18:1	h24:0	682.7	298.3	19.39	100	45	10.4
t18:1	h24:1	680.7	298.3	19.39	100	45	9.19
t18:1	h26:0	710.7	298.3	19.39	100	45	11.5
t18:1	h26:1	708.7	298.3	19.39	100	45	10.3
d18:0	h16:0	556.5	266.3	19.39	80	43	7.03
d18:0	h18:0	584.6	266.3	19.39	80	46	8.23
d18:0	h20:0	612.6	266.3	19.39	90	48	9.46
d18:0	h20:1	610.6	266.3	19.39	88	49	8.46
d18:0	h22:0	640.6	266.3	19.39	95	47	10.6
d18:0	h22:1	638.6	266.3	19.39	85	44	9.38
d18:0	h24:0	668.7	266.3	19.39	92	50	11.7
d18:0	h24:1	666.7	266.3	19.39	81	50	10.6
d18:0	h26:0	696.7	266.3	19.39	98	50	12.8
d18:0	h26:1	694.7	266.3	19.39	88	52	11.6
d18:1	h16:0	554.5	264.3	19.39	62	37	6.48
d18:1	h18:0	582.6	264.3	19.39	62	41	7.79
d18:1	h20:0	610.6	264.3	19.39	68	42	8.92
d18:1	h20:1	608.6	264.3	19.39	65	43	7.82
d18:1	h22:0	638.6	264.3	19.39	68	47	10.1
d18:1	h22:1	636.6	264.3	19.39	65	45	8.89
d18:1	h24:0	666.7	264.3	19.39	75	45	11.3
d18:1	h24:1	664.7	264.3	19.39	69	45	9.97
d18:1	h26:0	694.7	264.3	19.39	83	48	12.3
d18:1	h26:1	692.7	264.3	19.39	78	49	11.1

LCB	Fatty acid	[M+H] (*m*/*z*)	Product ion (*m*/*z*)	Dwell time (ms)	DP (V)	CE (V)	ET (min)
(D) Glucosylceramides							
d18:1	c12:0	644.5	264.3	19.39	90	50	2.58
t18:0	h16:0	734.6	300.3	19.39	80	68	3.38
t18:0	h18:0	762.6	300.3	19.39	80	68	3.86
t18:0	h20:0	790.6	300.3	19.39	80	72	4.68
t18:0	h20:1	788.6	300.3	19.39	80	75	4.27
t18:0	h22:0	818.7	300.3	19.39	80	60	5.87
t18:0	h22:1	816.7	300.3	19.39	80	63	4.66
t18:0	h24:0	846.7	300.3	19.39	80	60	6.89
t18:0	h24:1	844.7	300.3	19.39	80	65	5.83
t18:0	h26:0	874.7	300.3	19.39	80	63	7.98
t18:0	h26:1	872.7	300.3	19.39	80	65	6.77
t18:1	h16:0	732.6	298.3	19.39	88	49	3.14
t18:1	h18:0	760.6	298.3	19.39	70	54	3.47
t18:1	h20:0	788.6	298.3	19.39	70	55	4.65
t18:1	h20:1	786.6	298.3	19.39	75	60	3.96
t18:1	h22:0	816.7	298.3	19.39	88	57	5.59
t18:1	h22:1	814.7	298.3	19.39	75	60	4.67
t18:1	h24:0	844.7	298.3	19.39	100	57	6.52
t18:1	h24:1	842.7	298.3	19.39	100	59	5.50
t18:1	h26:0	872.7	298.3	19.39	100	57	7.54
t18:1	h26:1	870.7	298.3	19.39	100	62	6.39
d18:0	h16:0	718.6	266.3	19.39	85	56	3.87
d18:0	h18:0	746.6	266.3	19.39	85	80	6.17
d18:0	h20:0	774.6	266.3	19.39	93	80	7.57

(*Continues*)

DOI: 10.1002/rcm

Table 1. (Continued)

LCB	Fatty acid	[M+H] (*m*/*z*)	Product ion (*m*/*z*)	Dwell time (ms)	DP (V)	CE (V)	ET (min)
d18:0	h20:1	772.6	266.3	19.39	93	75	6.82
d18:0	h22:0	802.7	266.3	19.39	93	80	8.80
d18:0	h22:1	800.7	266.3	19.39	93	75	7.64
d18:0	h24:0	830.7	266.3	19.39	93	100	9.81
d18:0	h24:1	828.7	266.3	19.39	100	95	8.82
d18:0	h26:0	858.7	266.3	19.39	100	100	10.8
d18:0	h26:1	856.7	266.3	19.39	100	95	9.62
d18:1	h16:0	716.6	264.3	19.39	78	53	3.55
d18:1	h18:0	744.6	264.3	19.39	80	56	4.30
d18:1	h20:0	772.6	264.3	19.39	80	60	5.17
d18:1	h20:1	770.6	264.3	19.39	80	58	4.04
d18:1	h22:0	800.7	264.3	19.39	80	62	6.11
d18:1	h22:1	798.6	264.3	19.39	80	66	5.12
d18:1	h24:0	828.7	264.3	19.39	90	60	7.09
d18:1	h24:1	826.7	264.3	19.39	95	63	6.04
d18:1	h26:0	856.7	264.3	19.39	90	67	8.13
d18:1	h26:1	854.7	264.3	19.39	85	63	6.96

LCB	Fatty acid	[M+H] (*m*/*z*)	Product ion (*m*/*z*)	Dwell time (ms)	DP (V)	CE (V)	ET (min)
(E) Glycosylinositolphosphoceramides							
GM1		1546.9	366.1	19.39	145	50	6.07
t18:0	h16:0	1152.6	554.5	19.39	145	60	3.92
t18:0	h18:0	1180.6	582.5	19.39	145	60	4.96
t18:0	h20:0	1208.7	610.6	19.39	145	60	6.08
t18:0	h20:1	1206.7	608.6	19.39	145	61	5.12
t18:0	h22:0	1236.7	638.6	19.39	145	62.5	7.40
t18:0	h22:1	1234.7	636.6	19.39	145	61	6.32
t18:0	h24:0	1264.7	666.6	19.39	145	62.5	8.65
t18:0	h24:1	1262.7	664.6	19.39	145	62	7.74
t18:0	h26:0	1292.8	694.7	19.39	145	63	9.93
t18:0	h26:1	1290.8	692.7	19.39	145	63	9.00
t18:1	h16:0	1150.6	552.5	19.39	145	56	3.65
t18:1	h18:0	1178.6	580.5	19.39	145	58	4.67
t18:1	h20:0	1206.7	608.6	19.39	145	61	5.82
t18:1	h20:1	1204.7	606.6	19.39	145	60	4.77
t18:1	h22:0	1234.7	636.6	19.39	145	61	6.98
t18:1	h22:1	1232.7	634.6	19.39	145	60	5.89
t18:1	h24:0	1262.7	664.6	19.39	145	62	8.24
t18:1	h24:1	1260.7	662.6	19.39	145	63	6.96
t18:1	h26:0	1290.8	692.7	19.39	145	63	9.58
t18:1	h26:1	1288.8	690.7	19.39	145	65	8.15
d18:0	h16:0	1136.6	538.5	19.39	145	57	4.18
d18:0	h18:0	1164.7	566.6	19.39	145	57	5.16
d18:0	h20:0	1192.7	594.6	19.39	145	57	6.43
d18:0	h20:1	1190.7	592.6	19.39	145	57	5.21
d18:0	h22:0	1220.7	622.6	19.39	145	58	7.60
d18:0	h22:1	1218.7	620.6	19.39	145	58	6.50
d18:0	h24:0	1248.7	650.6	19.39	145	61	8.92
d18:0	h24:1	1246.7	648.6	19.39	145	61	7.56
d18:0	h26:0	1276.8	678.7	19.39	145	63	9.78
d18:0	h26:1	1274.8	676.7	19.39	145	63	8.79
d18:1	h16:0	1134.6	536.5	19.39	145	57	3.84
d18:1	h18:0	1162.7	564.6	19.39	145	57	4.78
d18:1	h20:0	1190.7	592.6	19.39	145	57	5.80
d18:1	h20:1	1188.7	590.6	19.39	145	57	4.85
d18:1	h22:0	1218.7	620.6	19.39	145	58	6.93
d18:1	h22:1	1216.7	618.6	19.39	145	58	5.87
d18:1	h24:0	1246.7	648.6	19.39	145	61	8.22
d18:1	h24:1	1244.7	646.6	19.39	145	61	7.01
d18:1	h26:0	1274.8	676.7	19.39	145	63	9.59
d18:1	h26:1	1272.8	674.7	19.39	145	63	8.20

DOI: 10.1002/rcm

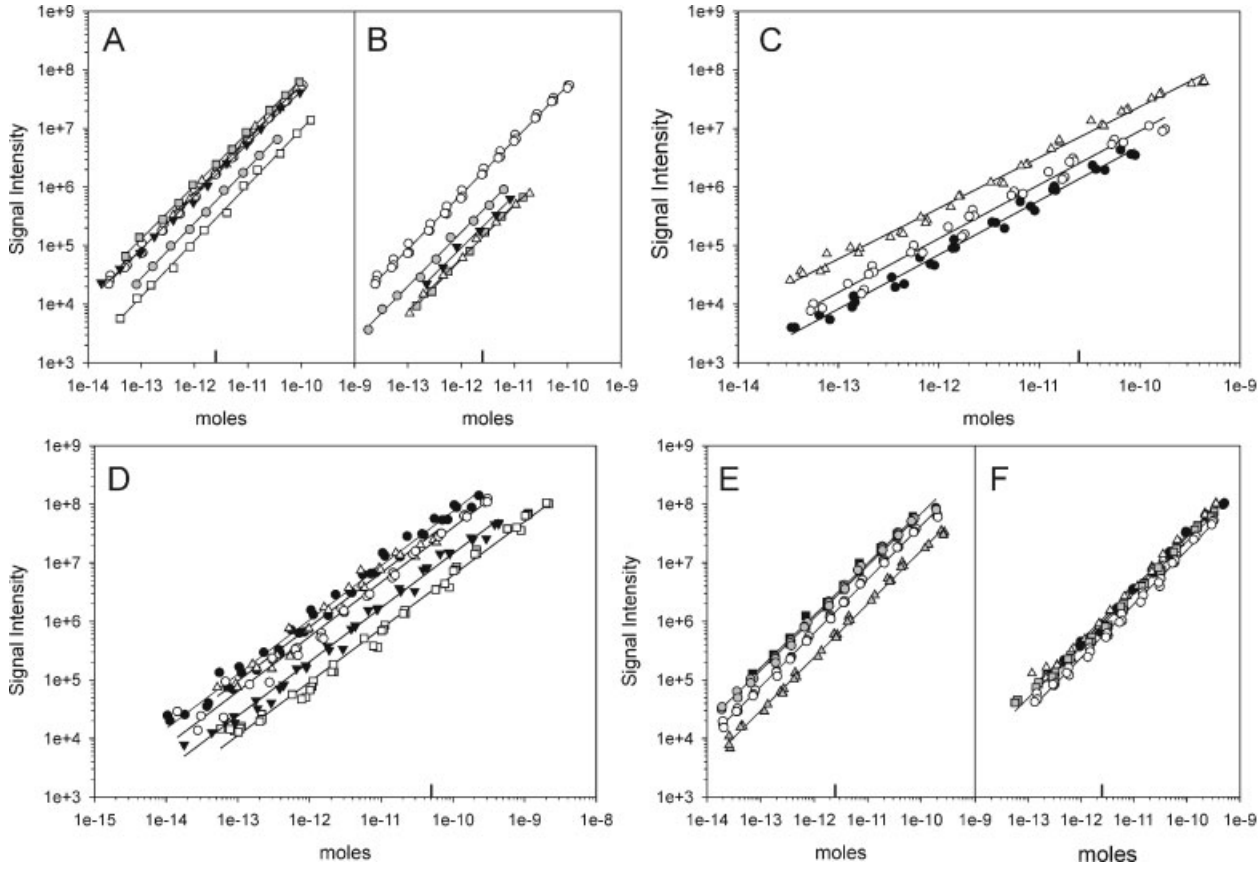

Figure 2. Standard curves for Arabidopsis sphingolipids and internal standards. Except where noted, all curves show only the linear portion for each standard and unknown. Unless specified, samples consisted of a mix of fatty acids with chain length from 16–26 carbon atoms. All scales are logarithmic. (A) Standard curves for synthetic and commercially purified animal ceramides: ○, C12 ceramide standard; ■, d18:1Δ4c16:0 ceramide; △, d18:1Δ4 ceramides; ▼, d18:1Δ4 hydroxyceramides; ●, d18:0c24:0 ceramide; □, t18:0c18:0 ceramide. (B) Standard curves for internal standard and purified plant ceramides. Higher concentrations of plant ceramides were not tested due to low amounts of purified compound: ○, C12 ceramide standard; ■, t18:1Δ8 ceramides; △, t18:0 ceramides; ▼, d18:1Δ8 hydroxyceramides; ●, d18:0 hydroxyceramides. (C) Standard curves for internal standard and purified plant glucosylceramides: △, d18:1Δ4c12:0 GlcCer standard; ●, d18:1Δ8 GlcCers; ○, t18:1Δ8 GlcCers. (D) Standard curves for ganglioside GM1 and purified plant GIPCs: □, GM1 standard; ●, t18:1Δ8 GIPCs; △, t18:0 GIPCs; ▼, d18:1Δ8 GIPCs; ○, d18:0 GIPCs. (E) Standard curves for LCBs: ■, d17:1Δ4; ○, d18:0, ▲, t18:0, ●, d18:1Δ4. (F) Standard curves for LCB-Ps: ●, d17:1Δ4-P; △, t18:0-P; ■, d18:1Δ4-P; ○, d18:0-P.

Table 2. LC/MS method properties. All gradients were pre-equilibrated at starting %B for 0.5 min plus the time for the autosampler injection cycle which made a total equilibration time of approximately 1 min. Start of the HPLC gradient was synchronized with the inline switching of the sample in the sample loop. At the end of the gradient the %B was increased to 100% over 1 min and held at 100% B for an additional 1 min to ensure complete elution of all compounds from the column before proceeding to the following gradient program

Analytes	Starting %B	End %B	Gradient time (min)
Glucosylceramides	50	70	10
Ceramides	40	75	14
Hydroxyceramides	40	75	14
GIPCs	25	50	10
LCBs & LCBPs	10	35	8

ganglioside GM_1 was used. As a result of the different chemistry of the standards to the sphingolipids being measured, the unknowns being quantified do not always give the same signal intensity on a mole-for-mole basis as the standard (Fig. 2). For example, in Fig. 2(A) the standard is a synthetic ceramide with a d18:1Δ4 LCB and a C12 fatty acid. When measuring other ceramides with a d18:1Δ4 LCB the mole-for-mole signal intensity was found to be nearly identical. However, when the ceramide being measured was a phytoceramide or a dihydroceramide the mole-for-mole signal intensity changed significantly. In order to account for the difference in signal intensity, a

DOI: 10.1002/rcm

RCM

Table 3. Signal intensity/mole factorials for each class of sphingolipid. Factorials were calculated to convert moles of standard into moles of analyte based on the calibration curves for each standard and class of analytes (Fig. 2). Factorials for certain compounds were unable to be determined (n/d) due to a lack of available purified sphingolipid and instead a value was estimated (in parentheses) based on the known abundance of the particular LCBs in these classes of sphingolipids[11] and on the behavior of the known compounds with similar chemistry

Class/LCB	d18:0	d18:1	t18:0	t18:1
Ceramides	3	4	6	5
Hydroxyceramides	3	4	6	5
Glucosylceramides	n/d (4)	6	n/d (4)	3
GIPCs	0.16	0.45	0.12	0.08
LCBs	2	1	5	n/d (4)
LCB(P)s	1.8	1	1	1

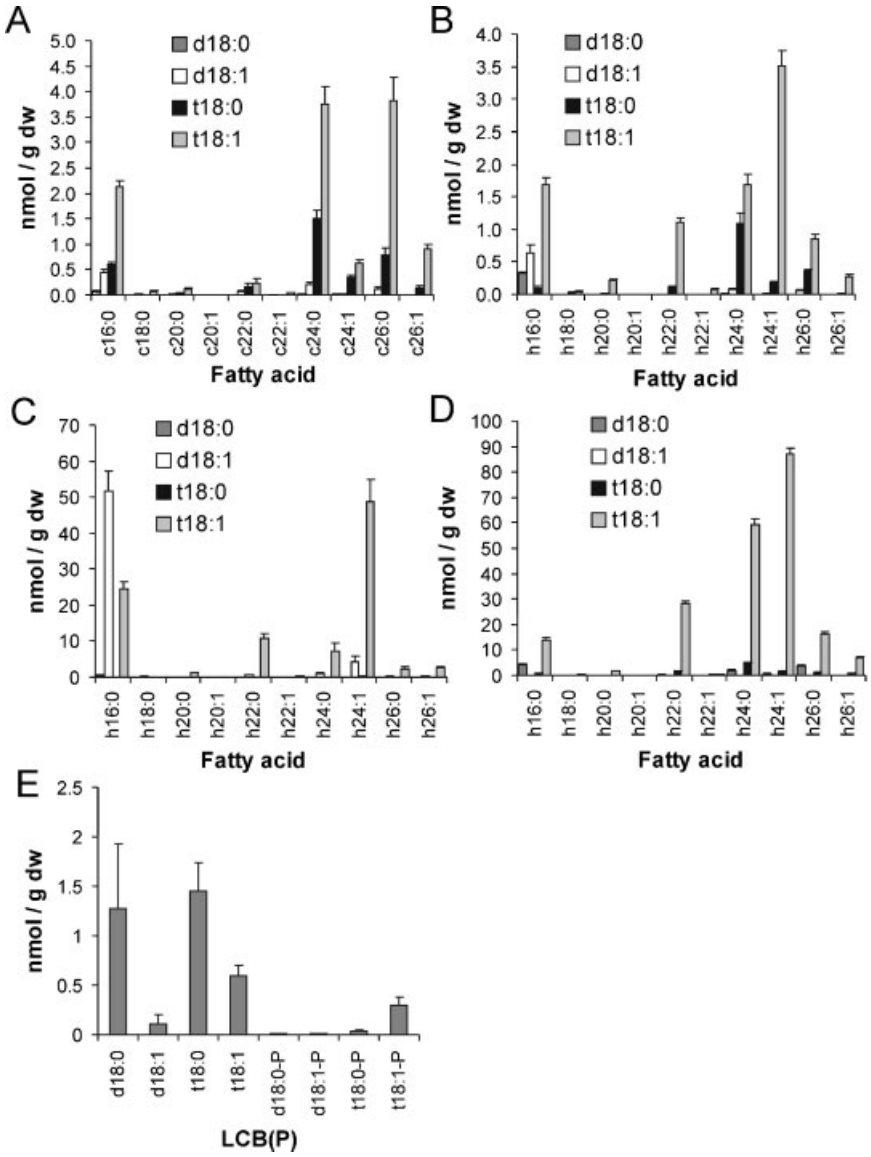

Figure 3. Sphingolipids detected in crude samples of *Arabidopsis thaliana* Col-0. Level of sphingolipids calculated by comparison to internal standards using the factorials in Table 3 and presented as grams per dry weight (g dw): (A) ceramides, (B) hydroxyceramides, (C) glucosylceramides, (D) GIPCs, and (E) LCB(P)s. Charts show average (n = 7) + one standard deviation.

DOI: 10.1002/rcm

Table 4. Comparison of methods for detection of plant sphingolipids. Previous methods for plant sphingolipid analysis involved separation of the sphingolipid classes and analysis of the sphingolipid content by hydrolysis and fluorescent derivitization and measurement of the liberated LCBs. These figures were previously published in g/fresh weight,[11] which is approximately one-tenth the amount in g/dw. Figures for LC/MS/MS are the total for each class of the different species shown in Fig. 3

Sphingolipid/method	Separation/LCB analysis	LC/MS/MS
Ceramide	13.7 nmol/g dw	16.3 ± 1.3 nmol/g dw
Hydroxyceramide		12.4 ± 0.8 nmol/g dw
Glucosylceramide	267 nmol/g dw	156 ± 15.3 nmol/g dw
GIPCs	501 nmol/g dw	236 ± 6.7 nmol/g dw
LCB(P)s	nd	3.8 ± 0.9 nmol/g dw
Total	782 nmol/g dw	425 ± 20.4 nmol/g dw

factorial was calculated for each sphingolipid chemistry that would place the regression line for each data set within the 99% confidence limits of the standard. These calculated factorials are shown in Table 3.

Method validation

In order to test the reproducibility of the method and measure the errors inherent in the procedure, seven identical extractions were made from a batch of freeze-dried, ground leaf tissue. An estimation of the total sphingolipid content of the tissue sample was made by hydrolyzing the total tissue and analyzing the released LCB content (2068 ± 100 nmol/g dw). After HPLC/MS the amount of sphingolipid in each sample was calculated based on the signal from the internal standard and the factorial shown in Table 3. This produced data for 168 sphingolipid species, which is presented in Fig. 3. The total amount of sphingolipid detected by LC/MS/MS was 425 nmol/g dw. This is in contrast to that detected by hydrolysis and LCB analysis of total tissue which is five times greater. However, the ratio of the different sphingolipid classes detected by LC/MS/MS is broadly consistent with that detected by separation and LCB analysis (Table 4) indicating that the method, while not without limitations, is a good indicator for the overall sphingolipid content.

DISCUSSION

Sphingolipids are bioactive lipids whose level within the cell may regulate cell fates. This makes the measurement of the level of sphingolipids an important part of understanding their biology. Plants may present a greater challenge than some other organisms for measuring sphingolipids due to the greater degree of heterogeneity found within the long-chain base component. For example, Arabidopsis has four different major long-chain bases compared to just two in yeast and animals. This increased heterogeneity makes identification of individual lipid species difficult by mass alone as several species have identical precursor and product masses under the conditions used here and interference from isotopes can also contaminate the signal of some species. These problems are circumvented in this method by using reversed-phase HPLC conditions that resolve individual sphingolipid species and prevent interference between peaks thereby providing an additional level of identification based on retention times.

A concern with separating compounds and standards using a gradient of solvent is that it may lead to changes in signal intensity depending on the solvent content at the time of the elution. However, most of the gradients described here were modest overall changes in solvent, the greatest being for elution of ceramides which involved a 14% increase in THF content at the expense of water which might be expected to have little effect on signal intensity. In support of this, in Fig. 2(A) the d18:1c12:0 standard curve matches exactly the d18:1c16:0 and d18:1c16-26 standards suggesting that elution time has little effect on signal intensity under the conditions employed here.

Despite a lack of truly authentic standards it is clear that similar standards can be used in their place if calibration curves are created to measure the difference in signal intensity. Although standards may have a high degree of structural similarity to the unknown it is clear that such curves are necessary for all sphingolipid variants within each class to be measured, as even minor changes in the structure of the LCB component, such as position of desaturation, affects the signal intensity/mole ratio. This is largely due to the ease with which the LCB component can undergo dehydration which is affected by saturation or hydroxylation at the 4-carbon position.

The resulting methods for detecting different classes of sphingolipids were found to be linear over 3 orders of magnitude or more enabling measurement of large changes in sphingolipid content. Such large changes are often found in mutant plants and in plants challenged with sphingolipid metabolism inhibitors (data not shown). The method is robust when measuring levels of sphingolipids that fall within the linear ranges described above. When measuring very low levels of sphingolipids the method becomes more prone to error as demonstrated by the large variance in the low-abundance sphingolipids (Fig. 3). This is mostly due to background effects. Background effects were reduced by using an X-type syringe for reduced carryover and an extended washing scheme for the autosampler with potent washing solvents; however, they could not be eliminated altogether and this is what determined the maximum sensitivity of the method.

In general, three repetitions per sample produced an acceptable level of variance for the most abundant sphingolipids. Increasing the number of repetitions did not greatly reduce the standard deviation for these measurements indicating the level of variance is inherent in the method. For less abundant sphingolipids, increasing the number of sample repetitions does reduce the variance and up to five repetitions may be necessary to detect two-fold changes in

DOI: 10.1002/rcm

RCM

the level of these sphingolipids; detection of smaller changes is most likely not feasible.

Although extensive calibration of the detected sphingolipids using authentic purified Arabidopsis sphingolipids was performed, the total amount of sphingolipid detected by LC/MS/MS falls short of that detected by other methods. The precise reason for this is not clear but the largest factor is most likely to be due to suppression of the efficiency of ionization in crude samples.[17] In support of this proposition, the signal intensity from the internal standard is reduced by a factor of up to ten-fold when combined with a crude extract (data not shown). This suppression of ionization is most likely caused by matrix effects – other compounds in the crude extract that interfere with ionization efficiency. In an attempt to reduce matrix effects crude extracts were dissolved in water-saturated butanol and washed with 0.1 N HCl in butanol-saturated water to remove polar compounds (data not shown); however, this had no effect on signal intensity suggesting that interfering matrix components are other hydrophobic compounds in the extract. One solution to this problem is to account for matrix effects by calibrating in the presence of an artificial matrix. However, the final quantification by LC/MS/MS is not often verified by other methods.[12,18]

Where LC/MS/MS is vastly superior to previous analytical methods, however, is in the amount of structural information acquired and the short sample preparation and analysis time. Previous methods for analysis of plant sphingolipids typically required extensive and time-consuming sample preparation and provided only a limited amount of information on the LCB content and or the fatty acid content of the hydrolyzed sample for three sphingolipid classes.[11] The current method is able to report what LCB/fatty acid combinations or molecular species are present and in what comparative quantity for 40 different LCB/fatty acid chain length combinations for four different sphingolipid classes, in addition to measuring free LCB and LCB-Ps. This entire measurement is possible from 300 mg fresh weight or less starting material with approximately 20 min hands-on sample preparation time and 1 h LC/MS/MS analysis time. This makes high-throughput analysis of plant sphingolipids a realistic proposition and should be applicable to deciphering the changes in plant sphingolipid content in a wide variety of mutants and in response to biological challenges.

Acknowledgements

This work was funded by NSF Arabidopsis 2010 grant, MCB 0312559. The Applied Biosystems 4000 QTRAP was funded by a NSF equipment grant, DBI 0521250. The authors thank Dr Ed Cahoon for his critical reading of the manuscript and our reviewers for their comments and recommendations.

REFERENCES

1. Borner GHH, Sherrier DJ, Weimar T, Michaelson LV, Hawkins ND, MacAskill A, Napier JA, Beale MH, Lilley KS, Dupree P. *Plant Physiol.* 2005; **137**: 104.
2. Mongrand S, Morel J, Laroche J, Claverol S, Carde JP, Hartmann MA, Bonneu M, Simon-Plas F, Lessire R, Bessoule JJ. *J. Biol. Chem.* 2004; **279**: 36277.
3. Liang H, Yao N, Song JT, Luo S, Lu H, Greenberg JT. *Genes Dev.* 2003; **17**: 2636.
4. Abbas HK, Tanaka T, Duke SO, Porter JK, Wray EM, Hodges L, Sessions AE, Wang E, Merrill AH, Riley RT. *Plant Physiol.* 1994; **106**: 1085.
5. Brandwagt BF, Mesbah LA, Takken FL, Laurent PL, Kneppers TJ, Hille J, Nijkamp HJ. *Proc. Natl. Acad. Sci. USA* 2000; **97**: 4961.
6. Spassieva SD, Markham JE, Hille J. *Plant J.* 2002; **32**: 561.
7. Ng CKY, Carr K, McAinsh MR, Powell B, Hetherington AM. *Nature* 2001; **410**: 596.
8. Cuvillier O, Pirianov G, Kleuser B, Vanek PG, Coso OA, Gutkind S, Spiegel S. *Nature* 1996; **381**: 800.
9. Maceyka M, Milstien S, Spiegel S. *Prostaglandins Other Lipid Mediat.* 2005; **77**: 15.
10. Lynch DV, Dunn TM. *New Phytologist* 2004; **161**: 677.
11. Markham JE, Li J, Cahoon EB, Jaworski JG. *J. Biol. Chem.* 2006; **281**: 22684.
12. Merrill AH Jr, Sullards MC, Allegood JC, Kelly S, Wang E. *Methods* 2005; **36**: 207.
13. Lester RL, Dickson RC. *Anal. Biochem.* 2001; **298**: 283.
14. Aveldano MI, Horrocks LA. *J. Lipid Res.* 1983; **24**: 1101.
15. Clarke NG, Dawson RM. *Biochem. J.* 1981; **195**: 301.
16. Sperling P, Heinz E. *Biochim. Biophys. Acta* 2003; **1632**: 1.
17. Annesley TM. *Clin. Chem.* 2003; **49**: 1041.
18. Bielawski J, Szulc ZM, Hannun YA, Bielawska A. *Methods* 2006; **39**: 82.

DOI: 10.1002/rcm